PRINT ISSN 1119-8362
Electronic ISSN 2659-1502

Full-text Available Online at
https://www.ajol.info/index.php/jasem
https://www.bioline.org.br/ja

J. Appl. Sci. Environ. Manage.
Vol. 27 (11) 2543-2551 November 2023

Sorption of Congo red Dye from Aqueous Solution by Mercerized and Benzoylated Sugarcane Bagasse: Isotherm, Kinetic and Thermodynamic Studies

***SAMUEL, AE; IDRIS, U; SAMAILA, DS; ALFA, TA; KAMBA, SY**

Department of Chemistry, Federal University of Agriculture, Zuru, Kebbi State-Nigeria

**Corresponding Author: seaadeiza@yahoo.com*
Co-Authors Email: idrisumar2010@gmail.com; bondesamaila@gmail.com; alfatijjaniabdulrahman@gmail.com; chemsky001@gmail.com

ABSTRACT: The use of large quantity of synthetic dye in process industries to colour products amongst other things has given rise to aqueous effluents containing high level of this pollutant. This paper therefore evaluates the use of isotherm, kinetic and thermodynamic to study the sorption capacities of congo red dye by mercerized sugarcane bagasse (MSB) and benzoylated sugarcane bagasse (BSB) in aqueous solution using batch experimental protocol. Data obtained show that MSB was the most effective adsorbent material, with equilibrium sorption (q_e = 13.64 mg/g) after 50 minutes. The optimum pH and dosage for dye uptake were 3.0 and 3.5 g respectively. Sorption of dye by the modified surfaces decreases with increasing temperature and ionic strength. The 4% NaOH presented the best desorption of dye on the adsorbents. Kinetic studies showed pseudo second-order model fit for the experimental data. Adsorption of the anionic dye on the modified surfaces fits the Langmuir isotherm model based on the R^2 values. Thermodynamic results showed ΔG^o values (-12.42 to -4.16 KJ/mol) for MSB and (-15.13 to -7.55KJ/mol) for BSB, consistent with the spontaneity and feasibility of the sorption process. The uptake of dye by the modified surfaces depicts a random nature at the solid-solution interface and showed that the sorption is exothermic as evidenced by value (0.256-0.334KJmol/K) and (-18.41 to -10.17 KJ/mol) for ΔS^o and ΔH^o respectively. The results present MSB and BSB as effective sorbent materials for removal of anionic dye from waste effluents.

DOI: https://dx.doi.org/10.4314/jasem.v27i11.25

Cite this paper as: SAMUEL, A. E; IDRIS, U; SAMAILA, D. S; ALFA, T. A; KAMBA, S. Y. (2023). Sorption of Congo red Dye from Aqueous Solution by Mercerized and Benzoylated Sugarcane Bagasse: Isotherm, Kinetic and Thermodynamic Studies. *J. Appl. Sci. Environ. Manage.* 27 (11) 2543-2551

Dates: Received: 30 September 2023; Revised: 29 October 2023; Accepted: 07 November 2023 Published: 30 November 2023

Keywords: Adsorption; Benzoyl peroxide; Dye; Kinetics; Sodium Hydroxide

Advancement in technological knowledge has given rise to large scale industrial activities, resulting in the upsurge of organic and inorganic pollutants from process industries. Contamination of water bodies by these pollutants has provoked worldwide interest in remediation methods to mitigate the harmful and environmental health hazards pose by these pollutants in eco-systems Cheng *et al.*, (2015). Textile, leather, rubber latex, food industries churn out immense volume of waste water containing reactive dye, disposal of these polluted waste waters into the eco-system without remediation could result in deleterious effects on human being Muhammad *et al.*, (2013). Hence, the sorption of dye from these colored waste effluents is imperative before discharging them into aquatic streams. Coloured dyes are classified namely; anionic, cationic and non-ionic dyes Ngulube *et al.*, (2017). Congo red dye is a dipolar benzidine- based diazo anionic molecule, which largely constitutes waste water effluents from dying, paper, textile, plastics, printing and rubber industries Yusef *et al.*, (2017). Stemming from its aromatic ringed structure, congo red dye is very stable and non-biodegradable Cheng *et al.*, (2015); Yusef *et al.*, (2017); Chatterjee *et al.*, (2010). Several physicochemical methods notably: electrochemical techniques, chemical

**Corresponding Author: seaadeiza@yahoo.com*

oxidation, coagulation-flocculation, ion-exchange, membrane separation and adsorption have been employed for remediation of congo red dye from waste streams Muhammad *et al.*, (2013) and Yusef *et al.,* (2017). Considerably, adsorption method has been given more attention owing to its high sorption capacity, eco-friendliness and efficiency. Because of its cellulosic nature, large surface area and low-cost, sugarcane bagasse has been used for the sorption of congo red dye in the form of bagasse fly ash Mall *et al.*, (2005), Ball-milled sugarcane bagasse Zhang *et al.*, (2011) and milled sugarcane bagasse Muhammad *et al.*, (2013). Similarly, glucose-amine copolymers and their composites: Chitosan Ngulube *et al.,* (2017), Chitosan/Montmorillonite nanocomposite Wang and Wang (2007) and clay-based materials namely; Kaolin Vimonses *et al.*, (2009), montmorillonite Yusef *et al.*, (2017), have been reported for the remediation of congo red dye from waste water and aqueous media. Sugarcane bagasse, a pulp or dry refuse left after juice has been extracted from sugarcane or sugarbeets, find uses as fuel, cattle feeds or starting material for paper making. This cellulosic based polymer is a low-cost, non-toxic, eco-friendly and high surface area material. This study investigates the use of isotherm, kinetic and thermodynamic studies on the sorption capacities of congo red dye by benzoyl peroxide and sodium hydroxide modified sugarcane bagasse in aqueous solution.

MATERIAL AND METHODS

Preparation of Adsorbent: The sugarcane bagasse used for this study was obtained from a sugarcane processing section of Zuru market Kebbi State, brought into the laboratory, washed under running water and dried (105ºC) in a thermostatic oven for 6 h. The dried sugarcane bagasse was milled using a jar mill (JM 4055) loaded with ceramic pebbles for 72 h and then fractionated (mesh: 75 micron) to obtained the fine sugarcane bagasse powdered material (SB).

Mercerization of Sugarcane Bagasse: 100 g sugarcane bagasse (SB) powder was weighed into a 500 ml beaker and 100 ml of 10% (w/v) NaOH solution was added. The mixture was equilibrated on a magnetic stirrer set at 150 rpm and 50ºC for 1 h. The beaker was cooled to room temperature and then filtered. The residue was then washed repeatedly with deionised water until neutral to litmus. The mercerized sugarcane bagasse (MSB) was then dried in an oven at 105ºC for 6h, cooled and packed into a polyethylene bag for sorption studies.

Benzoylation of Sugarcane Bagasse: 100 g of sugarcane bagasse powder was weighed into a 500 ml conical flask and 10 ml of toluene was added, the flask and its content were homogenized (100 rpm for 30 min.) on a flask shaker. The flask was then charged with 1% benzoyl peroxide compared to the weight of sugarcane bagasse powder (Sharma and Kundu, 2008). The flask and its content was then placed on a magnetic stirrer and heated at 120ºC with continous stirring (200 rpm) for 30 min. the benzoylated sugarcane bagasse (BSB) was then filtered and washed repeatedly with deionised water until neutral to litmus.

Characterization of Adsorbent: The sugarcane bagasse, mercerized sugarcane bagasse and benzoylated sugarcane bagasse were characterized physicochemically for their swelling ratio (Fieldson and Barbari, 1993), bulk density and pH of point zero charge (pH_{PZC}) (Soldatkina *et al.*, 2013; Soldatkina and Zavrichko, 2019). The spectrums of unmodified and modified sugar cane bagasse were obtained with Fourier Transform Infrared Spectroscopy (FTIR) spectrophotometer (Agilent) in a wave number range (500- 3500 cm^{-1}).

Effect of Initial Dye Concentration: 1.0 g MSB and BSB were studied separately with 20 ml of dye solutions (100, 150. 200, 250 and 300 ppm) in a 250 ml stopped conical flask. The flasks were agitated in a shaker at 200 rpm for 50 min., each flask was then filtered and the filtrate were analysed at a maximum wavelength of 490 nm using UV-Visible spectrophotometer for residual dye concentration. The amount of dye on the adsorbent material which represents the dye uptake was calculated from the equation Soldatkina and Zavrichko (2019).

$$q_e = \frac{(C_o - C_e)v}{m} \qquad 1$$

Where, C_O and C_e are the initial and final concentrations of dye solution, v is the volume of dye solution and m is the mass of sorbent materials.

Effect of Contact Time: 1.0 g of MSB was weighed into a 250 ml conical flask; 20 ml of 300 ppm dye solution was aggregated into the flask. The flasks were agitated (200 rpm) at different equilibration time (20, 30, 40, 50, 60, 70, 80 and 90 min.). The content of the flask was then filtered and the filtrate analyzed using UV-Visible spectrophotometer. The same experimental protocol was carried-out for the BSB sorbent material.

Effect of Adsorbent Dosage: MSB and BSB in various weights (1.0, 1.5, 2.0, 2.5, 3.0, 3.5, 4.0, 4.5, 5.0, 5.5 and 6.0g) were weighed separately into 250 ml conical flask. 20 ml of 300 ppm dye solution was aggregated into each flask and agitated (200 rpm) for 50 min. the content of flask was then filtered and the residual dye concentration determined. The amount of dye on the sorbent material at equilibrium time (q_e) was evaluated.

Effect of Temperature

1.0g of each sorbent material were weighed and aggregated with 20 ml of 300 ppm dye solution into a 250 ml conical flask. The flask was then mounted on a magnetic stirrer (200 rpm at 30^{o}C) for 50 min. this experiment was repeated at the same stirring speed and time, but with variation in temperature: 35, 40, 45 and 50^{o}C respectively. The residual dye concentration was determined and the value of q_e evaluated.

Effect of pH: 3.5g of adsorbent materials was weighed into a 250 ml conical flask, 20 ml of 300 ppm dye solution was added to each flask, and the pH was adjusted to 2. The content of the flask was agitated at 200 rpm for 50min. the mixture was then filtered, residual dye concentration determined and value of q_e evaluated. The same experimental procedure repeated, but with adjustment in pH to 3, 4, 6, 8 and 10, using 0.5 M HCl and 0.5 M NaOH as required.

Effect of Ionic Strength: The study was carried out by adding different amounts of NaCl (25 to 125 ppm of Na^+) into 20 ml of 300 ppm dye solution in conical flask containing 1.0g adsorbent material. The flask was agitated at 200 rpm for 50 min. the residual dye concentration were determined and q_e was subsequently calculated.

Desorption of Dye from Sorbent Material: The method Soldatkina and Zavrichko (2019) was used for the desorption studies. 1.0g of sorbent material was weighed into a 250 ml conical flask; 100 ml of 300 ppm dye solution was aggregated into the flask. The pH was adjusted to 3 and the flask was allowed to stand for 150 min. at room temperature. The sorbent material loaded with congo red dye was washed repeatedly with deionised water and dried at 50^{o}C. 0.1g of dye loaded material was weighed into a 250 ml conical flask, 10 ml of deionised water, 10 ml of 4% NaOH, 10 ml of 4% H_2SO_4 and 10 ml of methanol respectively were aggregated into each flask and agitated (200 rpm) at room temperature for 50 min. The efficiency of dye removal was calculated.

$$S(\%) = \frac{100(C_d \times V_d)}{q_e m} \qquad 2$$

Where, C_d is the dye concentration in solution after desorption, V_d is the volume of eluent, m is the mass of dye loaded material and q_e is equilibrium amount of dye adsorbed.

Isotherm studies: The data obtained in this study was fitted into three isotherms; Langmuir, Freundlich and Temkin.

$$\frac{C_e}{Q_e} = \frac{1}{K_L q_{\max}} + \frac{C_e}{q_{\max}} \qquad 3$$

Where, k_L, is the Langmuir constant, q_{max} is the quantity of adsorbate required to form a single monolayer per unit mass of adsorbent and Q_e is the amount adsorbed on unit mass of the adsorbent (Cheng *et al.,* 2015).

$$Inq_e = InK_F + n^{-1} InC_e \qquad 4$$

Where, k_F is the Freundlich constant related to the adsorption capacity, n^{-1} is the adsorption intensity.

$$q_e = \frac{RTInK_T}{b} + \frac{RTInC_e}{b} \qquad 5$$

Where, k_T is the Temkin equilibrium constant corresponding to the maximum binding energy and b, is the heat of adsorption (Soldatkina and Zavrichko, 2019).

Kinetic studies: Dye uptake rates, is best described using kinetic models which determines the residence time of adsorbate and the controlling mechanism of the adsorption of the adsorbate on the adsorbent material. The pseudo-first order kinetic can be expressed (Adegoke *et al.,* 2017) as

$$In(q_e - q_t) = Inq_e - K_1 t \qquad 6$$

A plot of ln (q_e-q_t) vs t generated a straight line. The amount of dye sorbed per gram of adsorbent at equilibrium (q_e) was determined from the intercept ln q_e and the slope gave the rate constant k_1.

The pseudo-second order kinetic model can be expressed Su *et al.,* (2014) as.

$$\frac{t}{q_t} = \frac{1}{K_2 q_e^2} + \frac{t}{q_e} \qquad 7$$

Where, q_e is the maximum sorption capacity, t is the time, q_t is the amount adsorbed at time t and k_2 is the equilibrium rate constant. Plot of t/q_t vs t, gives q_e^2 and k_2 from the slope and intercept respectively.

Thermodynamic Study: Fundamental thermodynamic parameters; Gibbs free energy (ΔG^o), enthalpy change (ΔH^o) and entropy change (ΔS^o) derivable from the study could help fully understand the controlling process and will largely determine the feasibility of dye sorption by the modified sugarcane bagasse. The following equations Akpomie and Dawodu (2015) and Soldatkina and Zavrichko (2019) described the thermodynamic parameters

$$\Delta G = \Delta H^0 - T\Delta S^0 \qquad 8$$

$$InK_D = \frac{\Delta S^0}{R} - \frac{\Delta H^0}{RT} \qquad 9$$

$$InK_D = \frac{C_a}{C_e} \qquad 10$$

Where, T, is the temperature in Kelvin, R is the ideal gas constant, k_D is the thermodynamic equilibrium constant. C_a and C_e are the concentrations of dye sorbed and the equilibrium concentration of the dye in solution. A plot of $\ln k_D$ vs 1/T yields ΔH^o and ΔS^o from the slope and intercept respectively.

RESULTS AND DISCUSSION

Table 1 below presents some physicochemical properties of the unmodified and modified adsorbent materials. The highest swelling ratio and bulk density values shown by MSB may not be unconnected with the largest surface area due to the decrystallization of glucose chain occasion by the breaking and sodium hydroxide salvation of glycosidic linkages. The high acidity as represented by BSB corroborates the combination of abstracted proton from the cellulosic backbone of SB by phenyl radical and the subsequent reaction of this proton with benzoyl radical resulting in the formation of benzoic acid Samuel *et al.*, (2019). The presence of this carboxylic acid on the surface of BSB is evidenced in the low pH_{pzc} value recorded for the adsorbent material. The slight acidity and alkalinity showed by SB and MSB presumably may be attributed to oxidation of fermented sugar on SB and presence of residual NaOH on MSB respectively.

Table 1: Physicochemical properties of unmodified and modified adsorbent materials

Adsorbent Material	Swelling Ratio (q_m)			Bulk Density (gcm^{-1})	pH_{pzc}
	4% NaOH	4% HCl	4% NaCl		
SB	1.06±0.02	0.85±0.06	0.36±0.03	0.10	6.2
MSB	2.14±0.01	1.61±0.04	0.96±0.07	0.16	7.4
BSB	1.71±0.05	1.13±0.03	0.48±0.05	0.22	5.8

The FT-IR spectra for the sugarcane bagasse (SB), mercerized sugarcane bagase (MSB) and benzoylated sugarcane bagasse (BSB) are shown in figures 1, 2 and 3 respectively. The O-H stretching vibration at 3324 cm^{-1}presents a stronger and broader peak than 3287 cm^{-1} for BSB, therefore substantiates the larger surface and presence of more OH adsorption site on MSB. The C-H (methylene group) stretching vibration at 2914 cm^{-1}were present in MSB and BSB, suggesting the increase in aliphatic carbon chain in modified materials. The stronger peak at 1718 cm^{-1} for BSB compared to 1595 cm^{-1} for MSB may be ascribed to stretching vibration from C=O (carbonyl group) of cellulose and hemicelluloses in the native SB and contributory stretching vibrations from COOH. The peak at 1625 cm^{-1} and the weak peak at 1155 cm^{-1} may be due to the deformation vibration for H-O-H bonds for surface adsorbed water as a result of the hygroscopic nature of the surface carboxylic acid and the presence of aromatic ring on BSB respectively.

Figure 4 below presents the effect of sorption of initial dye concentration by MSB and BSB. The equilibrium amount of dye adsorbed by the modified materials increased with increase in dye concentration. This is in agreement with the sorption of congo red dye by sugarcane bagasse and bambara shell Muhammad *et al.*, (2013), and adsorption of congo red dye with bagasse fly ash Rao *et al.*, (2006). However, the equilibrium quantity sorbed by MSB was slightly greater than BSB.

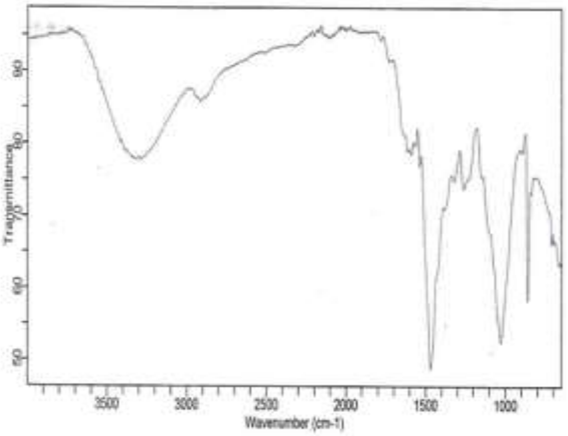

Fig 1: FT-IR spectrum of sugarcane bagase (SB)

The marginal increase may be attributed to the delignification of the lignocelluloses structure of sugarcane bagasse owing to alkaline hydrolysis, resulting in increased internal area and porosity of MSB adsorbent material.

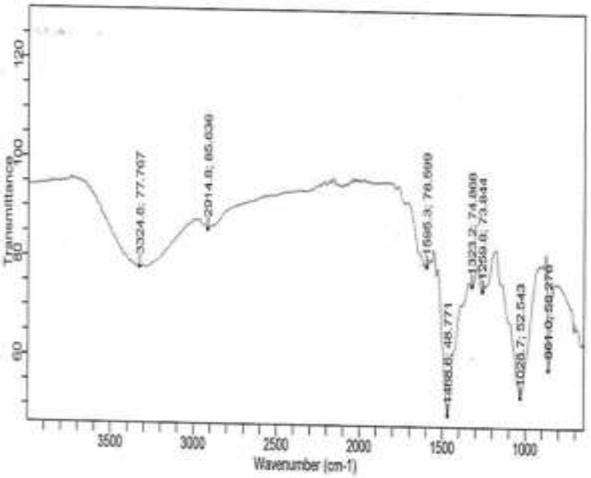

Fig 2: FT-IR spectrum of mercerized sugarcane bagasse (MSB)

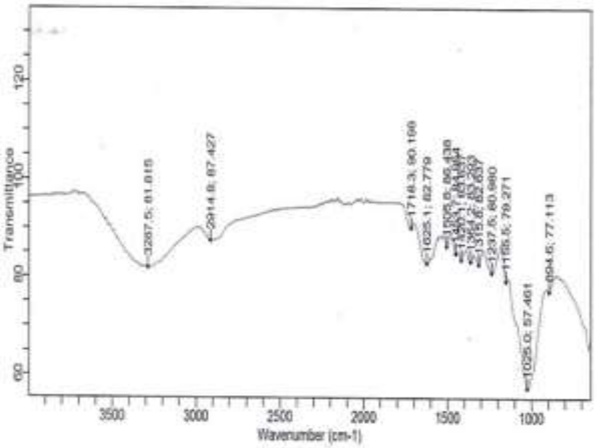

Fig 3: FT-IR spectrum of benzyolated sugarcane bagasse (BSB)

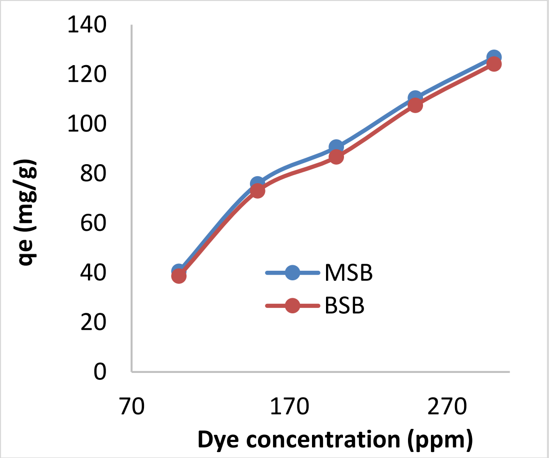

Fig 4: Effect of initial dye concentration.

The result of the batch experiment showing the effect of contact time is represented in figure 5. An increase in time brought about a concomitant increase in the equilibrium amount sorbed by the materials. Comparatively, at the equilibrium time of 50 min. for both materials, MSB and BSB showed equilibrium amount of 13.04 and 10.87 mgg^{-1} respectively. The relative sorption of adsorbate by MSB, suggest, that the alkaline treatment of the sugarcane bagasse resulted in decrystallization of glucose monomer and scissions of α-1,4 and β-1,6 glycosidic linkages present in the lignocellulosic material. Besides, the treatment of sugarcane bagasse with benzoyl peroxide may results in proton abstraction by the highly reactive benzoyl radical from cellulosic material and the subsequent formation of benzoic acid Penezek *et al.*, (2005) and Samuel *et al.*, (2019). The presence of this compound with aromatic ring and their preoccupation of active site, results in decreased dye sorption by BSB material.

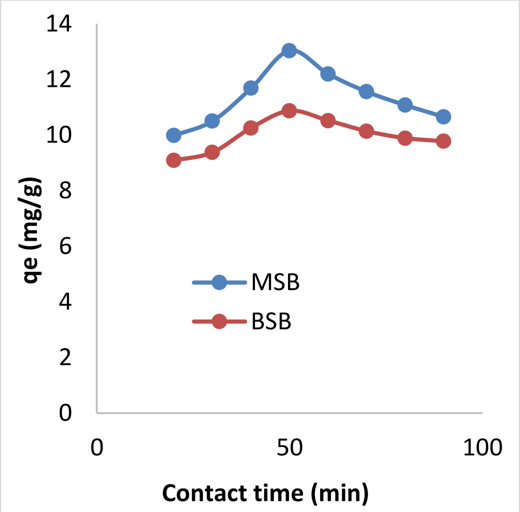

Fig 5: Effect of contact time on sorption capacity

The binding site available for sorption is determine, by the amount of sorbent material used Adegoke *et al.*, (2017). Figure 6, shows the effect of adsorbent dosage on the sorption of congo red dye by MSB and BSB. The percentage sorption increases with increase in adsorbent dosage, showing a peak at 3.5 g for both materials. Thereafter, incremental dosage of adsorbent results in decrease in the percentage of adsorbate uptake. This may be attributed to occupation of available binding sites by the dye molecules, such that a further increase in the quantity of MSB and BSB may not bring about any appreciable sorption of the adsorbate Zafer *et al.*, (2007) and Adegoke *et al.*, (2017). This result compares well with 4.0 g maximum adsorbent dosage reported for sugar cane bagasse and bambara shell (Muhammad *et al.*, 2013). Figure 7 shows the effect of pH on the sorption of congo red dye by MSB and BSB. pH of the dye solution is the most contributory factor that determines the surface chemistry of the adsorbent material and therefore, affects the adsorption of adsorbate by an adsorbent material Ozacar and Sengil (2003).

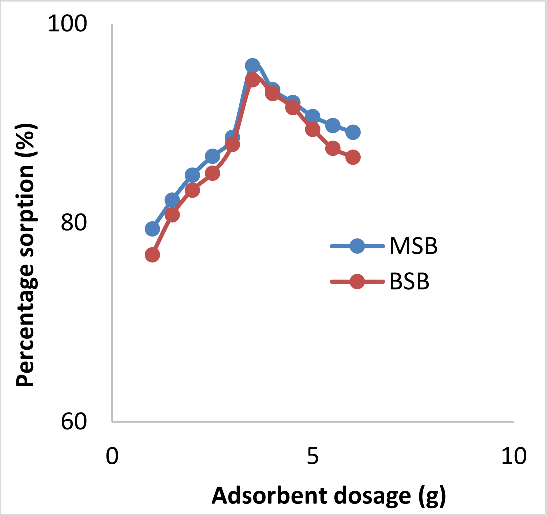

Fig 6: Effect of adsorbent dosage on dye sorption

The equilibrium quantity of the dye uptake increases from pH 2 to 3 and decreases thereafter. Congo red dye is a dipolar molecule, which exists as anionic molecule at basic pH and as cationic moieties at acidic pH Zhang *et al.*, (2011) and Muhammad *et al.*, (2013). At lower pH protonation of the nucleophilic (OH^-, COO^-) moieties on the adsorbent surfaces, enhances their affinity for the adsorbate, due to electrostatic attraction with their opposite charged groups present in the anionic dye molecule.

The increase in pH of the dye solution concomitantly increases OH^- in the dye solution resulting into competition for adsorptive sites on the adsorbent surfaces. Besides, the electrostatic repulsion between the negatively charge dye molecule and the negatively charge adsorbent surfaces contributes significantly to the decreased sorption of the dipolar molecule Malik, (2003), Tor and Cengeloglu, (2006) ; Muhammad *et al.*, (2013)

The effect of temperature on the sorption of dye molecule is presented in figure 8. The result showed that for both materials, the amount sorbed at equilibrium time decreases as temperature increases from 30 to 50 °C. Suggesting, an increase in temperature results in swelling of the biopolymer materials with associated desorption and possible diffusion of the dye molecules into the dye solution. The result from this study affirms the report of sorption of light green onto peanut husk modified by hexadecylpyridinium bromide Zhao *et al.*, (2017) and adsorption of methyl orange on wheat straw modified by cetyltrimethylammonium bromide Su *et al.*, (2014).

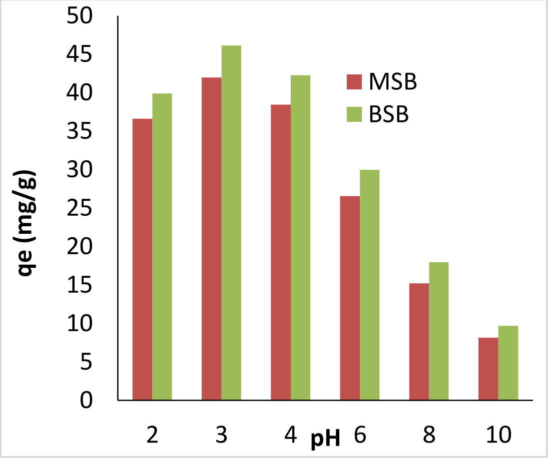

Fig 7: Effect of dye solution pH on sorption capacity

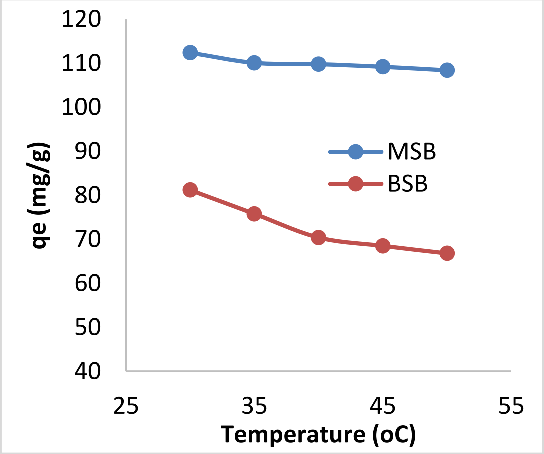

Fig 8: Effect of solution temperature on dye removal

The effect of the strength of electrolyte in dye solution is shown in figure 9. Sorption capacity of sorbent materials decreases marginally with a corresponding increase in strength of electrolyte. The dye uptake for MSB was higher than BSB this may be attributed to delignification and decrystalization of the cellulosic backbone by Sodium Hydroxide, resulting into a filamentous fibrous material with greater flexibility and improved sequesting of dye molecules. The decrease in dye uptake as the concentration of Na^+ increases may be attributed to the blocking of vacant sites by the electrolyte at a higher salt concentration Yusef *et al.*, (2017).

This is also in agreement with reports on removal of navy blue from aqueous solution by combined coagulation Nourmoradi *et al.*, (2016) and adsorption of congo red dye from aqueous solution by montmorillonite Yusef *et al.*, (2017). The slight decrease in dye uptake capacity as salt concentration increases suggest, that the modified materials could be an effective sorbent material of congo red dye from aqueous streams.

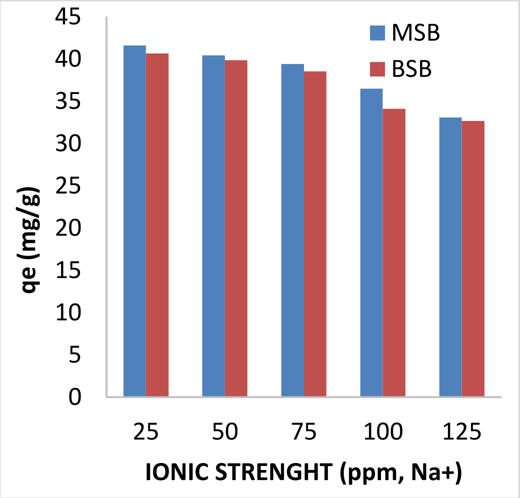

Fig 9: Effect of ionic strength on sorption capacity

Figure 10 represents the desorption of congo red dye using different solvents. The 4% H_2SO_4 showed the lowest desorption of the anionic dye from the sorbent materials. The highest desorption of dye by 4% NaOH indicates that reduction in positively charged adsorption sites in alkaline solution resulted in electrostatic repulsion of the dipolar molecule from the surfaces of the adsorbent materials Soldatkina and Zavrichko (2019). Besides, desorption of the anionic dye in excess by methanol more than distilled water and HCl may be attributed to entanglement of the dye molecules on the modified surfaces by ion-exchange or electrostatic attraction Su *et al.*, (2014).

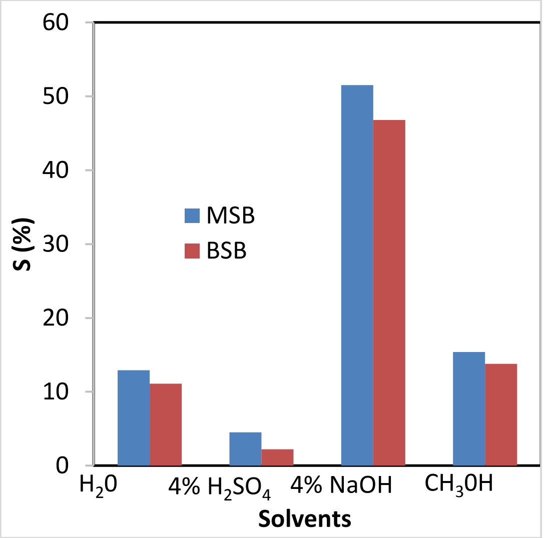

Fig 10: Effect of different eluents on dye desorption

The pseudo-first-order and pseudo-second-order kinetic model parameters of sorption of congo red dye onto MSB and BSB are presented in Table 2.

Table 2: Kinetic of dye sorption on the adsorbent materials

Kinetic Model	**Parameter**	**MSB**					**BSB**				
		303K	**308K**	**313K**	**318K**	**323K**	**303K**	**308K**	**313K**	**318K**	**323K**
Pseudo-first-order	**q_e**	7.25	6.90	6.66	6.81	6.14	6.47	6.21	6.08	6.11	5.92
	$K_1 \times 10^4$	2.66	3.01	3.55	3.72	4.44	1.98	2.04	2.09	2.92	3.31
	R^2	0.892	0.886	0.879	0.902	0.914	0.884	0.896	0.894	0.921	0.934
Pseudo-second-order	**q_e**	15.44	12.12	11.84	10.14	9.24	10.55	9.24	8.61	7.16	6.92
	$K_2 \times 10^3$	4.11	3.25	2.91	2.04	1.92	2.92	2.50	1.98	1.71	1.51
	R^2	0.999	0.997	0.995	0.998	0.996	0.994	0.992	0.996	0.999	0.998

Table 3: Isotherm parameters of dye uptake by adsorbent materials

Isotherm Model	**Parameter**	**MSB**					**BSB**				
		303K	**308K**	**313K**	**318K**	**323K**	**303K**	**308K**	**313K**	**318K**	**323K**
Langmuir	**q_{max}**	25.14	23.00	19.51	16.15	12.98	21.32	19.11	17.46	13.92	11.18
	K_L	0.061	0.058	0.052	0.048	0.043	0.053	0.049	0.044	0.039	0.036
	R^2	0.999	0.997	0.995	0.995	0.993	0.997	0.998	0.998	0.999	0.996
Freundlich	**n^{-1}**	0.46	0.44	0.42	0.40	0.43	0.53	0.51	0.50	0.48	0.45
	K_F	4.92	4.88	4.71	4.54	4.22	3.76	3.55	3.21	2.98	2.76
	R^2	0.886	0.876	0.868	0.889	0.885	0.899	0.888	0.879	0.894	0.869
Temkins	**K_T**	1.91	1.86	1.84	1.77	1.73	1.53	1.12	0.89	0.76	0.61
	b	485	506	541	653	692	462	490	497	561	596
	R^2	0.965	0.966	0.976	0.957	0.977	0.979	0.946	0.955	0.968	0.967

The low correlation value of R^2 as determined in pseudo-first-order model implies non applicability of this model. However, the high correlation values i.e. R^2= 0.995-0.999 for MSB and R^2=0.992-0.999 for BSB in the pseudo-second-order model indicates that chemosorption is the rate limiting step Soldatkina and Zavrichko (2019), and controls the mechanism for the sorption of congo red dye onto the modified surfaces. The results from this study affirm previous report on sorption of Acid Green and Acid Red on sawdust modified by cetyltrimethylammonium bromide Zhao *et al.,* (2017).

As shown in Table 3 above, the Langmuir, Freundlich and Temkins isotherms were used to describe the sorption of congo red dye onto MSB and BSB respectively. The highest correlation values of R^2= 0.993-0.999 for MSB and R^2= 0.996-0.999 for BSB as evidence in the Langmuir model, suggest better fit of the experimental data, indicating that the occupation of adsorption sites by the dipolar molecule was in form of a monolayer coverage Adegoke *et al.,* (2017). The Freundlich parameters 1/n and K_F decreases with increase in temperature for both sorbent materials, with correlation coefficient less than unity. The Temkins model shows a good linearity, judging by the correlation values of R^2 = 0.957-0.977 for MSB and R^2 = 0.955-0.979 for BSB. The good fitting of the data to Temkins isotherm suggest, a strong adsorbate-adsorbent interaction. In addition, the decreasing K_T value with temperature and positive value of b, which also increases with a corresponding, increase in temperature shows that adsorption of the dye molecule, was an exothermic process Soldatkina and Zavrichko (2019). This result is consistent with report from sorption of anionic dye on corn stalks modified by cetylpyridinium bromide Soldatkina and Zavrichko (2019), removal of congo red from aqueous solution by adsorption onto acid activated red mud Tor and Cengeloglu (2006), and biosorption of methyl orange from aqueous solutions using cationic surfactant-modified peanut husk in batch mode Su *et al.,* (2014).

Table 4: Thermodynamic parameters for the adsorbent materials

Adsorbent	ΔS° (KJmol/K)	ΔH° (KJ/mol)	ΔG (KJ/mol)				
			303 K	**308 K**	**313 K**	**318 K**	**323 K**
MSB	0.334	-18.41	-4.16	-6.51	-9.11	-10.31	-12.42
BSB	0.256	-10.17	-7.55	-8.16	-11.11	-13.44	-15.13

Table 4 represents the thermodynamic parameters for the adsorption of congo red dye by MSB and BSB adsorbent materials. The negative values of the enthalpy change (ΔH°), for all the adsorbents suggest, the exothermic nature of the sorption process. The positive values of the change in entropy (ΔS°), indicates an increase randomness of the dye uptake process, with increase in temperature, suggesting spontaneity of the sorption process Adegoke *et al.,* (2017) and Soldatkina and Zavrichko (2019), consistent with decrease in dye uptake as temperature of the dye solution increases.

Conclusion: Optimum conditions for the adsorption of the adsorbate by the modified surfaces were determined. The kinetic data described by the pseudo second-order model, fit better with the isotherms in the following order: Langmuir > Temkins > Freundlich. The modified surfaces demonstrate strong affinity for the dye molecule and showed that the sorption of the anionic dipolar molecule was spontaneous and feasible. This study shows that MSB and BSB could find practical applications in the remediation of congo red dye from waste streams.

REFERENCES

Adegoke, HI; Adekola, FA; Olowokere, IT; Yaqub, AL (2017). Thermodynamic studies on adsorption of lead (II) ion from aqueous solution using magnetite, activated carbon and composites. *J. Appl. Sci. Environ. Manage.* 3, 440-452.

Akpomie, KG; Dawodu, FA (2015). Potential of a low-cost bentonite for heavy metal abstraction from binary component system. *Chemosphere*: 4, 1-13.

Chatterjee, S; Lee, MW; Woo, SH (2010). Adsorption of congo red by chitosan Hydrogel Beads Impregnated with carbon nanotubes. *Bioresource Technol.* 101: 1800-1806.

Cheng, Z; Zhang, L; Guo, X; Jiang, X; Li, T (2015). Adsorption bahaviour of Direct red 80 and congo red on activated carbon/surfactant: process optimization, kinetics and Equilibrium. *Spectrochimica Acta part A: Mol. Biomole. Spect.* 137: 1126-1143.

Fieldson, GT; Barbari, TA (1993). The use of FTIR-ATR spectroscopy to characterize penetrant diffusion in polymers. *Polymers*: 34: 1146-1153.

Malik PK. (2003). Use of activated carbons prepared from saw-dust and rice husk for adsorption of acid dye. A case study of acid yellow 36. *Dyes pigment.* 56: 239-249.

Mall, I; Srivastava, V; Agarwal, N; Mishra, I (2005). Removal of congo red from aqueous solution by bagasse fly ash and activated carbon: kinetic study and equilibrium isotherm analysis. *Chemosphere*: 61: 492-501.

Muhammad, BI; Atika, MI; Haruna, MA; Maimuna, SY (2013). Removal of congo red dye from aqueous solution using sugarcane bagasse and bambara groundnut shell. *Chemsearch J.* 4(1): 22-28.

Ngulube, T; Gumbo, J; Masindi, M; Maity, A (2017). An update on synthetic dyes adsorption onto clay based minerals: A state-of-Art Review. *J. Environ. Manage*. 191: 35-57.

Nourmoradi, H; Zabihollahi, S; Pourzamani, HR (2016). Removal of a common textile dye navy blue (NB) from aqueous solutions by combined process of coagulation-flocculation followed by adsorption. *Desal. Water Treat*. 132: 212-220

Ozacar, M; Sengil, IA (2003). Adsorption of reactive dyes on calcined alunite from aqueous solutions. *J. Hazard. Mater*. 98: 211-224.

Penezek, P; Czub, P; Pielichowski, J. (2005). Unsaturated polyester resin: Chemistry and technology in crosslinking. *Material Science Ameduri. B. Ed. Springer-Verlag Berlin: Berlin*. 184:1-95.

Rao, VV; Rao, S; Ram, M (2006). Adsorption studies on treatment of textile dyeing industrial effluents by fly ash. *Chem. Engr. J.*: 116: 77-84.

Samuel, AE; Nwankwo, IC; Ezebor, F; Ojuolape, AA (2019). Adsorption of chromium by brewer's spent grain-g-poly (acrylic acid-co-acrylamide) from electroplating effluent. *Afr. J. Pure Appl. Chem*.4: 45-56.

Sharma V, Kundu PP. (2008). Condensation Polymers from Natural oils. *Prog. Polym. Sci*.33: 1199-1215.

Soldatkina, L; Zavrichko, M (2019). Equilibrium, kinetic and thermodynamic studies of anionic dyes adsorption on corn stalks modified by cetylpyridinium bromide. *Colloids. Interface*. 150: 200-213.

Soldatkina, LM; Menchuk, VV; Zavrichko, MA. (2013). Adsorption properties of polyaniline modified corn stalks. *Chemosphere.* 18: 13-19.

Su, Y; Jiao, Y; Duo, C; Han, R (2014). Biosorption of methyl orange from aqueous solutions using cationic surfactant-modified wheat straw in batch mode. *Desal. Water Treat*. 52: 6145-6156.

Tor, A Cengeloglu Y. Removal of congo red from aqueous solution by adsorption onto acid activated red mud. *J. Hazard. Mater*. 2006: 138:409-415.

Vimonses V, Lei S, Jin B, Chow C, Saint C. Kinetic study and equilibrium isotherm analysis of congo red adsorption by clay minerals. *Chem. Engr. J* .2009: 148: 354-364.

Wang L, Wang A. Adsorption characteristics of congo red onto chitosan/montmorillonite nanocomposite. *J. Hazard. Mater*. 2007: 147:979-985.

Yusef OK, Hassan B, Heshmatollah N, Mohammad JM, Ahmad RY, Shahram S, Abdeltif A. Adsorption of congo red dye from aqueous solutions by montmorillonite as a low-cost adsorbent. *Inter. J. Chem. React. Engr*. 2017: 201: 16-27.

Zafer MN, Nadeem R, Hanif MA. Biosorption of nickel from protonated rice bran. *J. Hazard. Mater.* 2007: 143: 478-485.

Zhang Z, Moghaddem L, O'Hara IM, Doherty WOS. Congo red adsorption by ball-milled sugarcane bagasse. *Chem. Engr. J*. 2011: 178: 122-128.

Zhao B, Xiao W, Shang Y, Zhu H, Han R (2017). Adsorption of light green anionic dye using cationic surfactant-modified peanut husk in batch mode. *Arab. J. Chem.* 2017: 10: 3595-3602.